



Material Behaviour

Correlating chemical and physical changes of photo-oxidized low-density polyethylene to the activation energy of water release

Shiran Garnai Hirsch^{a,b}, Boris Barel^a, Dina Shpasser^c, Ester Segal^{a,**}, Oz M. Gazit^{c,*}^a Department of Biotechnology and Food Engineering, Technion – Israel Institute of Technology, Haifa 3200003, Israel^b Netafim Ltd., D.N Hefer, 38845 Israel^c Department of Chemical Engineering, Technion – Israel Institute of Technology, Haifa 32000, Israel

ARTICLE INFO

Keywords:

Photo-oxidation

Modulated thermal gravimetric analysis

(MTGA)

Carbonyl index

Low-density polyethylene

ABSTRACT

Understanding and quantifying the effect of degradation on the chemical and physical properties of LDPE films is crucial for maintaining high quality of recycled LDPE products. Thermal gravimetric analysis coupled with mass spectroscopy (TGA-MS), Fourier transform infrared spectroscopy (FTIR), differential scanning calorimetry and electron microscopy combined with modulated TGA (MTGA) were used to evaluate LDPE films that sustained natural and accelerated weathering. Cross-referencing the chemical changes occurring to the LDPE samples during the weathering process with the dynamic results of MTGA provided a strong correlation between the release of caged water from the bulk of the LDPE and a specific energy value (E'), termed here as 'volitalization energy'. The E' value and the temperature at which it is measured are shown, for the first time, to be descriptors for the extent of photo-degradation. The data for accelerated- and naturally-induced degradation show a similar trend with respect to the effect of UVA radiation. A strong correlation is shown between the extent degradation determined by the traditional carbonyl index and the rate of water evaporation at the E' temperature.

1. Introduction

Exceptional thermal and chemical properties combined with excellent processability are what makes polyethylene (PE) one of the most extensively used synthetic polymers [1]. Unfortunately, the highly stable chemical structure of PE is also what makes it not biodegradable, resulting in the accumulation of huge amounts of post-usage waste [2]. The weathering of PE is known to have a strong damaging effect on its chemical and mechanical properties, leading in many cases to early application failure [3–5]. Hence, much emphasis is placed on mitigating these negative effects in an effort to extend the service life of PE-based products and substantially increase the use of recycled PE [6]. This has stimulated much research into the understanding and quantification of the governing photo-oxidative degradation processes and their effect on the micro and macro scale of PE⁷.

Modulated thermal gravimetric analysis (MTGA), first introduced by Blaine and Hahn in 1998, was developed as a tool to obtain continuous kinetic information on the decomposition processes of polymers [8,9]. The technique is based on an oscillating temperature program superimposed on a linear heating profile, which produces a sine wave force function. In this method, the rate of mass change is continuously

measured as a function of the oscillating temperature generating local maximum and minimum temperature values (termed as 'peaks' and 'valleys'). Using these values, the continuous activation energy curve is plotted according to equation (1) [7]:

$$E = \frac{RT_p T_v \ln(d\alpha_p/d\alpha_v)}{T_p - T_v} \quad (1)$$

where $d\alpha_p$ is the mass rate-of-change ($\% \text{ min}^{-1}$) at the temperature (T_p) where the peak is found and $d\alpha_v$ is the mass rate-of-change ($\% \text{ min}^{-1}$) at the temperature (T_v) where the valley is found. For more details regarding this equation please see Supporting Information, Equations S1-S2, and ASTM E2958 [10].

In traditional MTGA, multiple cycles of the sine wave are collected to plot the continuous activation energy curve, see Fig. 1. From the plateau region in the continuous energy curve we can calculate the activation energy for LDPE decomposition (E) [9]. As can be seen in Fig. 1, there are two sharp peaks at the onset and offset of the continuous activation energy curve. The most current claim is that these two sharp points are unrealistically high, and hence do not have any physical meaning [7,8].

Herein, we used the MTGA method to study the photo-degradation effect on low-density PE (LDPE) and evaluate the change in E values.

* Corresponding author.

** Corresponding author.

E-mail addresses: esegal@technion.ac.il (E. Segal), ozg@technion.ac.il (O.M. Gazit).

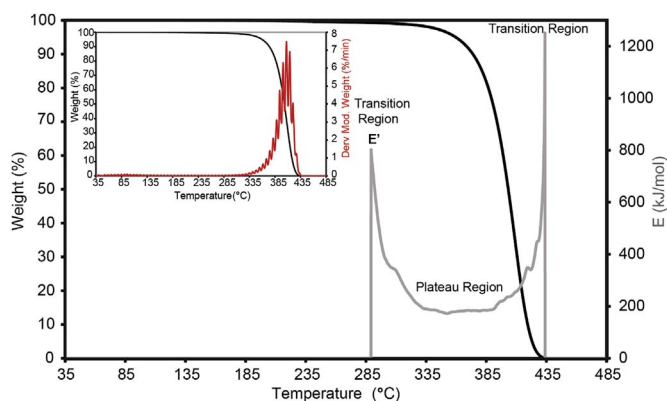


Fig. 1. Modulated thermogram (black trace) and the corresponding continuous activation energy curve (gray trace) for neat LDPE (un-weathered control sample). The inset depicts the corresponding modulated derivative.

Surprisingly, we find that the photo-degradation process has no effect on the traditionally calculated E values [11–17], neither under natural nor under accelerated weathering conditions. In contrast to what is currently perceived, we show here that the extent of LDPE photo-degradation is linearly correlated to the onset value associated with the measured activation energy curve. Analyzing the properties of LDPE using MTGA and TGA-mass spectrometry (TGA-MS) we show that this measured activation energy onset corresponds to the energy needed for the volatilization of water molecules locked within the polymer framework. We further show that the amount of water lost at a specific onset value is correlated with the value of the carbonyl index (CI), which is traditionally used to evaluate the extent of photo-degradation. We therefore term the energy value measured at the onset of the continuous activation energy curve as the E' , the energy of volatilization.

2. Experimental section

2.1. Preparation of LDPE films

LDPE samples (Ipethene 4203 by Carmel Olefins Ltd. Haifa, Israel), without stabilizing additives, with a MFI of 0.2 g/10 min and a density of 0.92 g cm⁻³ were used in this study. Thin films (50 ± 2 μm thick) were produced using a 30 mm single-screw extruder (L/D ratio of 30:1 with a screw speed of 120 rpm) equipped with a film blowing line (Labtech Engineering, Thailand). The die temperature was adjusted to 210 °C and the blown ratio was 2.5.

2.2. Weathering conditions

The LDPE films were weathered under natural and accelerated conditions. For natural weathering (NW), the films were exposed on the roof of our laboratory at Kibbutz Magal, Israel, for a period of four months (March–July 2015). Specimens were fixed in a custom-built setup, in which the films were positioned facing south at an angle of 45° with respect to the ground. The temperature, relative humidity and total irradiance were continuously recorded during exposure. Accelerated weathering (Acc) was conducted in a QUV tester (Q-Lab, USA) and the films were exposed to UVA irradiance (1.55 W m⁻²) at 60 °C with natural humidity created by the presence of an open water bath. No humidity cycles were performed. The weathered films were removed at designated time intervals for subsequent characterization.

2.3. Characterization

2.3.1. Modulated thermal gravimetric analysis (MTGA)

MTGA analysis was carried out using a TGA Q5000 IR (TA Instruments, USA) according to ASTM E2958-14 [10]. For each

measurement, a sample of 3.8 ± 0.3 mg, consisting of 6 small circular films (50 ± 2 μm thick and 5 mm in diameter), was placed in a “flower shape” arrangement within a platinum pan to obtain optimal heat transfer. The sample was first conditioned at 35 °C under nitrogen atmosphere (99.999%) for 30 min at a flow rate of 25 mL min⁻¹ and subsequently heated from 35 °C up to 500 °C at a rate of 2 °C min⁻¹ under nitrogen. The temperature modulation amplitude was ± 5 °C for a period of 200 s. To reduce statistical error, three independent measurements were carried out for each sample. Following each test the TGA pan was cleaned by heating under air. The activation energy (E) and pre-exponential factor ($\log Z$) were calculated using the TA universal analysis software. Notably, the specific set of parameters used here for the MTGA analysis were obtained following an optimization process conducted using the method described by Blaine and Hahn, for more details see Refs. [9,18]. The interested reader is referred to section 2 and Fig. S3 in the SI for more details on the parameter selection for the LDPE sample used here.

2.3.2. Thermal gravimetric analysis-coupled with mass spectrometry (TGA-MS)

TGA-MS experiments were carried out using a LABSYS Evo TGA (Setaram, France) coupled to a QGA mass spectrometer (Hiden Analytical, England), monitoring molecular species with 1–200 m/z. The QGA was equipped with two detectors; Faraday cup and SEM (secondary electron multiplier). Samples (12 ± 2 mg) were first conditioned at 35 °C under argon atmosphere (99.999%) for 30 min at a flow rate of 25 mL min⁻¹, and subsequently heated from 35 °C to 500 °C at a rate of 2 °C min⁻¹ under argon. The discharge gas was transferred to the QGA through a capillary gas connection heated to 210 °C by applying a vacuum of 10⁻⁶ torr. TGA data was analyzed using Calisto thermal analysis software and the MS data was analyzed using the MASsoft 7.

2.3.3. Fourier transform infrared - attenuated total reflectance (FTIR-ATR)

Samples were measured on a Thermo 6700 FTIR instrument equipped with a DTGS-detector and a diamond ATR device (Smart iTR). Spectra were collected at a range of 500–4000 cm⁻¹ and the instrument resolution was set to 4 cm⁻¹ with 16 scans per spectrum. For each sample, at least 5 independent measurements were collected.

2.3.4. Differential scanning calorimetry (DSC)

DSC measurements were performed using a Mettler-Toledo DSC-1 instrument equipped with HSS7 - High Sensitivity Sensor. For analysis, LDPE samples (5.2 ± 0.3 mg) were placed in 40 μl sealed aluminum pans and measured under nitrogen atmosphere at a flow rate of 25 mL min⁻¹. Measurements consisted of the following four sequential steps: (1) heating from -10 °C to 160 °C, (2) sample maintained at 160 °C for 3 min, (3) cooling to -10 °C and (4) heating to 160 °C. All steps were carried out a constant rate of 10 °C min⁻¹. The degree of crystallinity (X_c) was calculated using the following equation:

$$X_c = \frac{\Delta H_m}{f_p \Delta H_m^0} \quad (2)$$

where, ΔH_m is the latent fusion heat, f_p is the LDPE weight fraction, and ΔH_m^0 is the theoretical latent heat of fusion for 100% crystalline LDPE (293 J g⁻¹) [19].

2.3.5. High resolution scanning electron microscopy (HRSEM)

The morphology of the films was studied using a Zeiss Ultra-Plus Schottky field emission gun SEM (FEG-SEM) system operated at 1 keV. For cross-section analysis the films were cryogenically fractured in liquid nitrogen. To minimize charging effects samples were gold sputtered (Polaron sputter coater E5150) prior to imaging.

3. Results and discussion

The MTGA curve of the neat LDPE (un-weathered control sample) shows a single weight loss process at a temperature range of 190–435 °C, see Fig. 1. According to prior literature [20,21] and our TGA-MS studies (data not shown), under N₂ flow this mass loss is associated with the decomposition of LDPE and release of volatile hydrocarbons species, mainly C_nH_{2n}, n ~ 4–14. The sinusoidal heating process induced a modulated derivative weight curve, presented in the inset of Fig. 1. This modulated thermogram was used to calculate the continuous activation energy curve using Equation (1). Fig. 1 shows that below 290 °C and above 435 °C there is no weight change, i.e. $d\alpha_p/d\alpha_v = 0$, rendering the activation energy undefined, please refer to Fig. S1 and the related equation in the Supporting Information for a more detailed explanation. The initial value of the activation energy curve is observed as a sharp peak at a temperature of 290 °C, with a corresponding value of 800 kJ mol⁻¹. A second sharp peak is observed at 435 °C, with a corresponding value of 1250 kJ mol⁻¹, designating the end of mass loss. The formation of the two peaks is the result of the mathematical dependence of the continuous activation energy curve on the weight loss, see Supporting Information. Historically, these values marked the “transition regions” [18], in which the activation energy had insufficient data for proper deconvolution. At the temperature range between 350 °C and 390 °C the curve can be observed to plateau at a value of ~190 kJ mol⁻¹. This value fits well with the ‘activation energy’ (*E*) for LDPE decomposition, as reported by Flynn and Wall in their MTGA studies [9,22].

Performing a similar analysis for LDPE samples that have undergone different extent of weathering, either induced or natural, we found similar main features in the continuous activation energy curve. Fig. 2 presents the modulated thermograms and the corresponding continuous activation energy curves for LDPE films following accelerated weathering for different exposure durations. Interestingly, all samples were found to exhibit a plateau value of 190 kJ mol⁻¹ at the same temperature range, regardless of the extent of weathering. Distinctly, we found that *E'*, the energy obtained for the first transition peak, and the temperature at which it appears was highly dependent on the weathering duration and the weathering conditions, for more details refer to Fig. S2 in the Supporting Information. For example, the *E'* value for LDPE sample that was weathered for 504 h is 428 kJ mol⁻¹, which is 372 kJ mol⁻¹ lower than that of the un-weathered control LDPE. Furthermore, the *E'* for the 504 h-weathered sample appears at a temperature of 153 °C, which is lower by 138 °C than that of the un-weathered control LDPE sample. The trends in *E'*, shown in Fig. 2, led us to postulate that the *E'* value and the temperature at which it appears may have a thermodynamic interpretation.

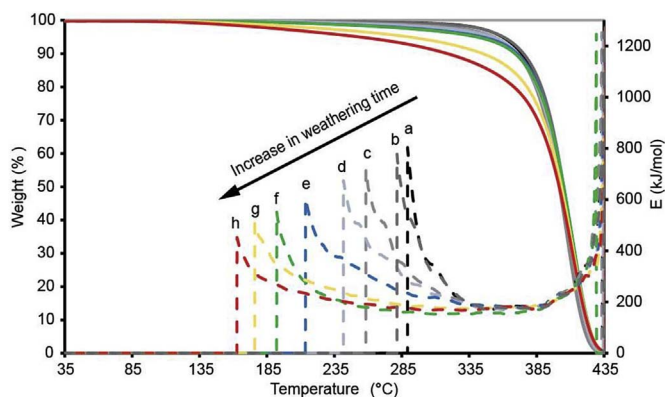


Fig. 2. Modulated thermograms and the corresponding continuous activation energy curve for LDPE films under induced weathering (UVA 1.55 W m⁻² at 60 °C) for different exposure periods (a = 0 h (control), b = 72 h, c = 144 h, d = 216 h, e = 288 h, f = 360 h, g = 432 h, h = 504 h).

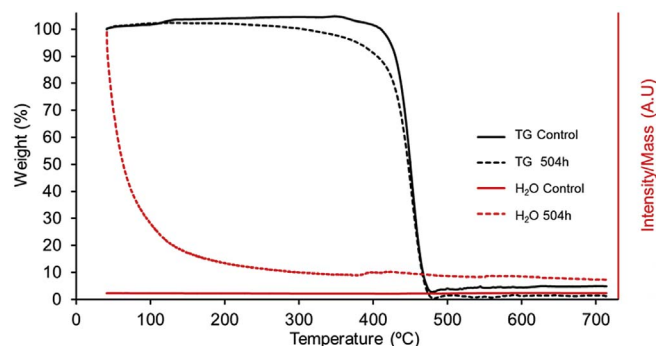


Fig. 3. Thermograms (black trace) and corresponding MS signal of H₂O (red trace, intensity normalized to sample mass) for un-weathered control LDPE film (t = 0 h) and a sample weathered for 504 h (UVA 1.55 W m⁻² at 60 °C). (For interpretation of the references to colour in this figure legend, the reader is referred to the web version of this article.)

To investigate this further, we performed extensive TGA-MS studies in order to identify chemical species that were released at the temperature range where *E'* appears. For clarity, Fig. 3 presents the data only for the two extreme samples t = 0 h (un-weathered control sample) and t = 504 h. For each sample, the temperature for the first transition region, designated as *E'*, was characterized by a 1–2% mass loss. During the TGA analysis, we scanned a range of mass-to-charge ratio (m/z) values to look for potential volatiles. Our analysis showed that only water (m/z = 18) and traces of CO₂ (m/z = 44) were released from the film during heating prior to the complete decomposition region. It can be seen in Fig. 3 that, for the control sample (t = 0), there is hardly any water release, which is consistent with the lack of oxygen in the sample and the inert carrier gas. However, the weathered LDPE films (t = 504 h) exhibited a significantly higher release of H₂O and a trace of dissolved CO₂, starting at a temperature as low as 50 °C. The degradation by exposure to UVA radiation is known to form free radicals within the polymer matrix. These radical species cause chain scission and react with oxygen from air to generate polar side groups, such as –OH, C=O, COOH and COO⁻, on the backbone of the polymer matrix [23–26].

More specifically, at early stages of LDPE photo oxidative degradation, the alkyl radicals react with atmospheric oxygen to form alkyl peroxy radicals. These radicals further react to form ketone groups followed by β-scission [27]. Prior literature has shown that photo-oxidative degradation of LDPE occurs via a convoluted reaction mechanism, which follows the Norrish Type I (N-I) and Norrish Type II (N-II) [28]. In short, the N-I involves the direct scission of the bond adjacent to an excited carbonyl group, with the formation of two radicals leading to the formation of terminal alcohol and carboxyl acid groups. The N-II proceeds through a chain scission without producing radicals leading to the formation of vinylidenes and aldehydes [29].

The FTIR-ATR spectra for the Acc and NW, as a function of weathering time, and the specific band assignments are provided in Fig. 4 and Fig. S4, respectively. Analysis of the data related to Acc samples, Fig. 4a, shows that the band at 3438 cm⁻¹, corresponding to the stretching vibrations of ν(O–H) in the formed hydroperoxides and alcohols [23,24,30,31], increases as a function of the weathering duration. Additionally, increasing amounts of carbonyl complexes were found to appear in the region of 1800–1650 cm⁻¹. This range contains a combination of overlapping individual bands attributed to specific groups such as aldehydes (1740–1733 cm⁻¹), carboxylic acid groups (1708–1698 cm⁻¹), ketones 1714 cm⁻¹ (1723–1713 cm⁻¹) and lactones (1786–1780 cm⁻¹) [23,31–42]. A third band was found to grow with weathering duration at 1170 cm⁻¹, typically assigned to ν(C–O) stretching vibrations in ether, carboxyl and hydroxyl groups [23,31]. The increase in the amount of unsaturated hydrocarbon groups appear as vinyl group at 910 cm⁻¹ [25, 26, 34].

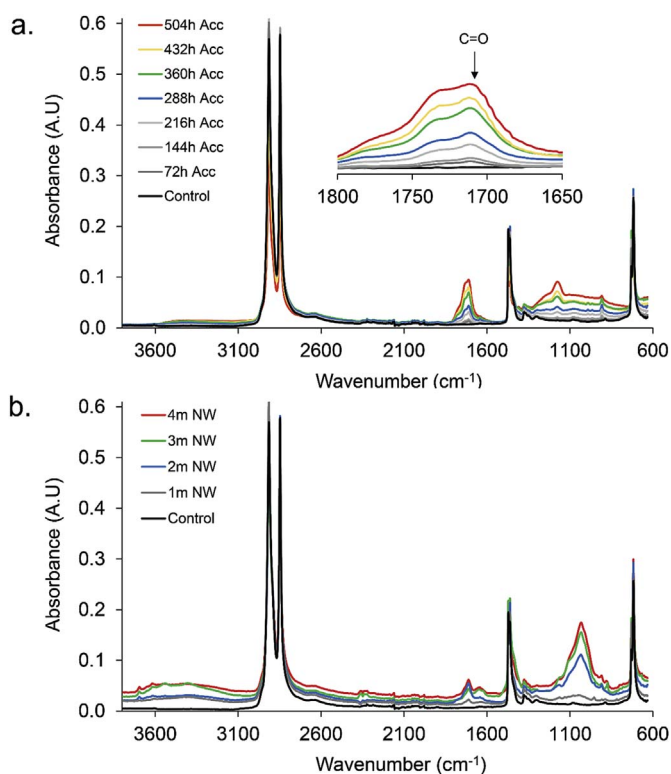


Fig. 4. FTIR-ATR spectra of LDPE films under (a) accelerated weathering (UVA 1.55 W m⁻² at 60 °C) and (b) natural weathering for different exposure durations.

As can be expected, the NW samples also showed an increase in the amount of hydrophilic side groups with increase in weathering duration, Fig. 4b. However, the specific bands that form in the NW samples were different from the Acc samples. The NW samples show the formation of a complex carbonyl band at 1780–1708 cm⁻¹, an ester band at 1180–1169 cm⁻¹, a dominant ether band at 1140–940 cm⁻¹, a wider hydroxyl groups at 3800–3050 cm⁻¹ and a relatively moderate formation of the carbonyl band. In addition, the NW samples showed the formation of a vinylidene band at 880 cm⁻¹.

The differences between the degradation mechanism of the Acc and the NW sample, measured by FTIR, are attributed to the different conditions under which the samples were weathered. It seems that, under the conditions used here in the Acc, the N-I mechanism was more dominant than the N-II mechanism, while in the NW the N-II mechanism was the dominant one. Irrespective of the specific degradation path, both N-I and N-II mechanisms lead to the production of hydrophilic side groups on the LDPE backbone, as can clearly be seen in the FTIR-ATR analysis in Fig. 4. This is consistent with the higher content of water in the Acc and the NW weathered LDPE samples, as compared to the control samples.

When plotting the values of E' as a function of weathering time (see Fig. 5a), either for accelerated or natural weathering, we find excellent linear correlation. Moreover, a similar observation can be made when plotting the E' onset temperature (termed as T') as a function of weathering duration, see Fig. 5b. The rate of degradation in the samples that sustained accelerated weathering was 10-fold faster than the rate of the samples that were weathered under natural conditions. Interestingly, we find that the ratio between the slope obtained for E' and that of T' as function of weathering time, under both accelerated, $dE'_{Acc}(t)/dT(E'_{Acc})$, and natural conditions, $dE'_{NW}(t)/dT(E'_{NW})$, is equal. This supports our hypothesis that the values of E' and T' originate from intrinsic thermodynamic changes sustained by the LDPE during the weathering process. Cross-referencing the MTGA results with those of the TGA-MS, showing that mostly water molecules were released before the main decomposition, we define E' as the ‘volatilization energy’ for

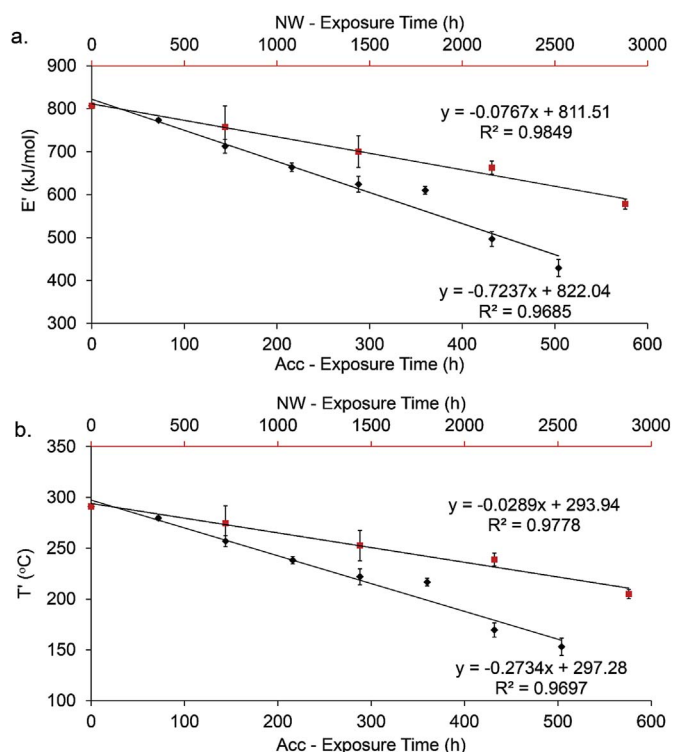


Fig. 5. (a) E' and (b) T' (E' onset temperature) values vs. weathering time under accelerated and natural conditions. Data are the average of 3 independent measurements for each sample.

removal of water. As mentioned above, the presence of water is due to the presence of hydrophilic side groups, which become more abundant with the weathering duration.

As demonstrated above, the value for E' was extracted from a gravimetric analysis (MTGA) that followed the water loss by diffusion from the bulk of the weathered LDPE samples. The diffusion of water from the LDPE bulk is a dynamic process, which is strongly dependent on the chemical and physical properties of the sample. As changes to the microstructure of the polymer, such as crystallinity and porosity, are well known to be temperature dependent, it is important to study these effects on the how E' -values.

The effect of weathering/degradation on the crystallinity of LDPE was assessed by out differential scanning calorimetry (DSC) measurements. It is known that the degradation process of LDPE depletes tie chains and amorphous regions with an associated recrystallization causing an increase in the degree of crystallization, X_c [43–51]. The results, summarized in Table 1, show that the degree of crystallization increases with the weathering duration. The differences in the X_c values are observed to be more pronounced when calculated from the enthalpy of melting of the first heating cycle rather than the values obtained from

Table 1
Degree of crystallinity (X_c) values of LDPE films after different accelerated weathering durations, as calculated from the DSC 1st and 2nd heating runs.

| Weathering duration (h) | X_c (%) | |
|-------------------------|-------------------------|-------------------------|
| | 1 st heating | 2 nd heating |
| 0 | 24.3 | 26.9 |
| 72 | 28.7 | 26.9 |
| 144 | 30.3 | 27.6 |
| 216 | 32.9 | 28.2 |
| 288 | 36.1 | 29.4 |
| 360 | 34.3 | 28.4 |
| 432 | 37.3 | 29.5 |
| 504 | 38.0 | 29.0 |

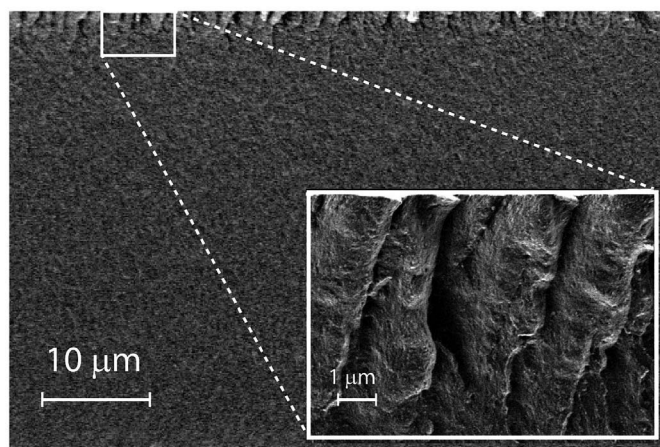


Fig. 6. Cross-sectional HRSEM image of LDPE sample, which was weathered for 504 h under UVA 1.55 W m^{-2} at 60°C .

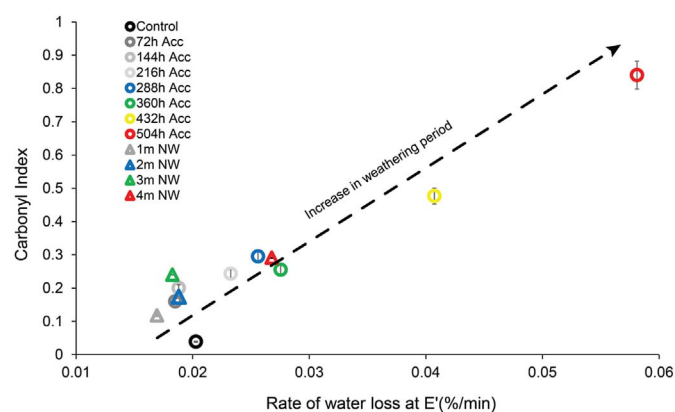


Fig. 7. Carbonyl index vs. % rate of water loss at E' for different exposure durations of accelerated weathering (UVA 1.55 W m^{-2} at 60°C). Note that error bars are included and represent data from 3 independent measurements.

the second heating cycle. It is well established that chain scission is more pronounced with longer exposure duration of the LDPE films to photo-oxidative conditions [52–54], which is measured as a decrease in the polymer molecular weight. Thus, in the samples that sustained longer duration of weathering, the LDPE chains are of lower molecular weight, and hence have higher degree of mobility. This in-turn enhances the overall crystallinity of the sample while it recrystallizes in the cooling step between the 1st and 2nd cycles [5,25]. The higher crystallinity of the degraded samples is well-known to be also accompanied by an increase in the LDPE brittleness [55]. This in turn results in the formation of cracks in the skin of the LDPE film, see HRSEM images in Fig. 6. The increase in the brittleness of the sample with the duration of weathering correlates well with the decrease in the energy of volatilization E' . Presumably, the increase in sample cracking can be ascribed to the enhanced diffusion of water out from the bulk of the LDPE film, thus lowering the energy needed to release these trapped water molecules. It can be inferred that, with the increase in weathering duration, the presence of hydrophilic side groups is extended deeper into the bulk of the LDPE. Hence, as the weathering duration increases, the water molecules may reside deeper into the bulk of the LDPE film. This will enhance the diffusion length for the water molecules and in turn the energy needed for their removal.

Traditionally, the extent of photo degradation is evaluated using the well-established parameter of the carbonyl index, which defined as the ratio between the integrated band absorbance of the carbonyl at 1714 cm^{-1} and that of the LDPE bending vibration of methylene (1463 cm^{-1}), and is conventionally used to characterize the degree of

oxidation of PE [24,31,35,56–59]. The data obtained for the carbonyl index (CI) of the weathered sample is plotted here as a function of the rate of mass loss (%) at E' , see Fig. 7. As can be seen, the accelerated weathering these two independent measurements and techniques, FTIR vs. MTGA, show a good correlation, which strongly supports our findings. The extent of degradation as measured by the CI for both the NW and Acc samples are shown to be well correlated with the trend obtained by MTGA. It is further evident that the NW samples exhibit relatively low degradation as compared to the Acc samples, consistent with the 10 fold lower E' values shown in Fig. 5.

4. Conclusions

We show that chemical and physical changes occurring during the degradation process of LDPE are correlated to the energy needed to initiate the removal of water from the bulk of the LDPE. Quantitatively, the energy and the temperature that represent the extent of degradation were measured by MTGA. The water volatilization energy, termed here as E' , is shown to be a descriptor for the extent of degradation. We show that E' is strongly correlated with the brittleness degree of the LDPE films and energy needed for water volatilization through the cracks and crazes. Analysis shows similar trends for both accelerated and natural weathering with a constant factorial ratio between the two types of exposures. It is shown that the value of E' can provide a quantitative measure for the extent of degradation of bulk LDPE samples, that cannot be analyzed using conventional spectroscopic methods.

Acknowledgements

The authors would like to gratefully acknowledge help of Dr. Anita Vaxman from Bazan Group for contributing the raw LDPE samples and Netafim LTD. laboratories for the natural and accelerated weathering services.

Appendix A. Supplementary data

Supplementary data related to this article can be found at <http://dx.doi.org/10.1016/j.polymeresting.2017.10.005>.

References

- [1] J.A. Brydson, *Plastics Materials*, Butterworth-Heinemann, 1999.
- [2] B. Singh, N. Sharma, *Polym. Degrad. Stab.* 93 (3) (2008) 561–584.
- [3] M. Kaci, T. Sadoun, K. Moussaceb, N. Akroune, *J. Appl. Polym. Sci.* 82 (13) (2001) 3284–3292.
- [4] S. Al-Salem, *Mater. Des.* 30 (5) (2009) 1729–1736.
- [5] T. Ojeda, A. Freitas, K. Birck, E. Dalmolin, R. Jacques, F. Bento, F. Camargo, *Polym. Degrad. Stab.* 96 (4) (2011) 703–707.
- [6] D.M. Wiles, G. Scott, *Polym. Degrad. Stab.* 91 (7) (2006) 1581–1592.
- [7] R. Blaine, *J. Test. Eval.* 42 (6) (2014) 1–6.
- [8] R.L. Blaine, *Method and apparatus of modulated-temperature thermogravimetry*, 6 (336) (2002) 741.
- [9] R. Blaine, B. Hahn, *J. Therm. Analysis Calorim.* 54 (2) (1998) 695–704.
- [10] Y. Javadi, M.S. Hosseini, M.K.R. Aghjeh, *Iran. Polym. J.* 23 (10) (2014) 793–799.
- [11] T. Ozawa, *Bull. Chem. Soc. Jpn.* 38 (11) (1965) 1881–1886.
- [12] J.H. Flynn, L.A. Wall, *J. Res. Nat. Bur. Stand* 70 (6) (1966) 487–523.
- [13] J. Flynn, *J. Therm. Analysis Calorim.* 27 (1) (1983) 95–102.
- [14] J. Foreman, C. Lundgren, P. Gill, In measurement of the physical properties of engineering thermoplastics using thermal analysis, technical papers of the annual technical conference-society of plastics engineers incorporated, 1993 Society of Plastics Engineers Inc, 1993, p. 3025.
- [15] L. Křizanovský, V. Mentlik, *J. Therm. Analysis Calorim.* 13 (3) (1978) 571–580.
- [16] H.L. Friedman, *J. Macromol. Science—Chemistry* 1 (1) (1967) 57–79.
- [17] H.L. Friedman, In Kinetics of thermal degradation of char-forming plastics from thermogravimetry. Application to a phenolic plastic, *J. Polym. Sci. Part C Polym. Symposia* 1964 (1964) 183–195 Wiley Online Library.
- [18] C.G. Slough, *J. Test. Eval.* 42 (6) (2014) 1–12.
- [19] B. Wunderlich, *Thermal analysis of Polymeric Materials*, Springer Science & Business Media, 2005.
- [20] J.A. Conesa, A. Marcilla, R. Font, J. Caballero, *J. Anal. Appl. pyrolysis* 36 (1) (1996) 1–15.
- [21] P. Rizzarelli, M. Rapisarda, S. Perna, E.F. Mirabella, S. La Carta, C. Puglisi, G. Valenti, *J. Anal. Appl. Pyrolysis* 117 (2016) 72–81.

- [22] ASTM Standard E1641-16, Standard Test Method for Decomposition Kinetics by Thermogravimetry Using the Ozawa/Flynn/Wall Method, American Society for Testing of Materials, West Conshohocken, 2016, pp. 1–7.
- [23] A. Kondyurin, I. Kondyurina, M. Bilek, *Polym. Degrad. Stab.* 98 (2013) 1526–1536.
- [24] J. Gulmine, P. Janissek, H. Heise, L. Akcelrud, *Polym. Degrad. Stab.* 79 (3) (2003) 385–397.
- [25] A. Corti, S. Muniyasamy, M. Vitali, S.H. Imam, E. Chiellini, *Polym. Degrad. Stab.* 95 (6) (2010) 1106–1114.
- [26] L. Guadagno, C. Naddeo, V. Vittoria, G. Camino, C. Cagnani, *Polym. Degrad. Stab.* 72 (1) (2001) 175–186.
- [27] A. Tidjani, *Polym. Degrad. Stab.* 68 (3) (2000) 465–469.
- [28] S.S. Fernando, P.A. Christensen, T.A. Egerton, J.R. White, *Polym. Degrad. Stab.* 92 (12) (2007) 2163–2172.
- [29] P. Roy, P. Surekha, C. Rajagopal, S. Chatterjee, V. Choudhary, *Polym. Degrad. Stab.* 92 (6) (2007) 1151–1160.
- [30] B. Fayolle, X. Colin, L. Audouin, J. Verdu, *Polym. Degrad. Stab.* 92 (2) (2007) 231–238.
- [31] A. Benítez, J.J. Sánchez, M.L. Arnal, A.J. Müller, O. Rodríguez, G. Morales, *Polym. Degrad. Stab.* 98 (2) (2013) 490–501.
- [32] P.K. Roy, P. Surekha, C. Rajagopal, S.N. Chatterjee, V. Choudhary, *Polym. Degrad. Stab.* 91 (8) (2006) 1791–1799.
- [33] P.K. Roy, P. Surekha, C. Rajagopal, V. Choudhary, *Polym. Degrad. Stab.* 91 (9) (2006) 1980–1988.
- [34] E. Chiellini, A. Corti, S. D'antone, R. Baciú, *Polym. Degrad. Stab.* 91 (11) (2006) 2739–2747.
- [35] B. Suresh, S. Maruthamuthu, A. Khare, N. Palanisamy, V. Muralidharan, R. Ragunathan, M. Kannan, K.N. Pandiyaraj, *J. Polym. Res.* 18 (6) (2011) 2175–2184.
- [36] J. Gulmine, L. Akcelrud, *Polym. Test.* 25 (7) (2006) 932–942.
- [37] M. Sugimoto, A. Shimada, H. Kudoh, K. Tamura, T. Seguchi, *Radiat. Phys. Chem.* 82 (2013) 69–73.
- [38] M.A. Ruhul, B.F. Abu-Sharkh, M. Al-Harathi, *J. Chem. Eng.* 27 (1) (2013) 74–77.
- [39] M. Wang, P. Wu, S.S. Sengupta, B.I. Chadhary, J.M. Cogen, B. Li, *Industrial Eng. Chem. Res.* 50 (10) (2011) 6447–6454.
- [40] H. Qin, Z. Zhang, M. Feng, F. Gong, S. Zhang, M. Yang, *J. Polym. Sci. Part B Polym. Phys.* 42 (16) (2004) 3006–3012.
- [41] A. Dehbi, A. Bouaza, A. Hamou, B. Youssef, J.M. Saiter, *Mater. Des.* 31 (2) (2010) 864–869.
- [42] B. Youssef, A.E. Dehbi, A. Hamou, J.M. Saiter, *Mater. Des.* 29 (10) (2008) 2017–2022.
- [43] N. Brooks, A. Unwin, R. Duckett, I. Ward, *J. Macromol. Sci. Part B Phys.* 34 (1–2) (1995) 29–54.
- [44] J. Feijoo, J. Sanchez, A. Müller, *Polym. Bull.* 39 (1) (1997) 125–132.
- [45] H. Springer, A. Hengse, G. Hinrichsen, *Colloid Polym. Sci.* 271 (6) (1993) 523–528.
- [46] X.R. Xu, J.T. Xu, L.X. Feng, *Polym. Int.* 51 (5) (2002) 458–463.
- [47] G. Spathis, E. Kontou, *J. Appl. Polym. Sci.* 91 (6) (2004) 3519–3527.
- [48] M. Niaounakis, E. Kontou, *J. Polym. Sci. Part B Polym. Phys.* 43 (13) (2005) 1712–1727.
- [49] A. Manzur, J.I. Rivas, *J. Appl. Polym. Sci.* 104 (5) (2007) 3103–3111.
- [50] G.-F. Shan, W. Yang, M.-B. Yang, B.-H. Xie, Q. Fu, Y.-W. Mai, *J. Macromol. Sci. Part B* 48 (4) (2009) 799–811.
- [51] N. Brooks, R. Duckett, I. Ward, *Polymer* 33 (9) (1992) 1872–1880.
- [52] J. Pabiot, J. Verdu, *Polym. Eng. Sci.* 21 (1) (1981) 32–38.
- [53] T. Kumayaka, R. Parthasarathay, M. Jollands, I. Ivanov, *Korea Aust. Rheol. J.* 22 (2010) 173–177.
- [54] D. Feldman, *J. Polym. Environ.* 10 (4) (2002) 163–173.
- [55] Y.-C. Hsu, M.P. Weir, R.W. Truss, C.J. Garvey, T.M. Nicholson, P. Halley, *J. Polym. Sci.* 53 (12) (2012) 2385–2393.
- [56] L. Tang, Q. Wu, B. Qu, *J. Appl. Polym. Sci.* 95 (2) (2005) 270–279.
- [57] J.M. Klein, G. Roberto Ramos, A.M. Coulon Grisa, R. Nichele Brandalise, M. Zeni, *Prog. Rubber, Plastics Recycl. Technol.* 29 (1) (2013) 39–54.
- [58] D. Klepac, M. Ščetar, G. Baranović, K. Galić, S. Valić, *Radiat. Phys. Chem.* 97 (2014) 304–312.
- [59] R. Yang, J. Zhao, Y. Liu, *Polym. Degrad. Stab.* 98 (2013) 2466–2472.